Journal of Catalysis **196,** 195–199 (2000)
doi:10.1006/jcat.2000.3028, available online at http://www.idealibrary.com on IDEAL®

RESEARCH NOTE

Distinction between Surface and Bulk Oxidation of Cu through N_2O Decomposition

Satoshi Sato,[1] Ryoji Takahashi, Toshiaki Sodesawa, Ken-ichi Yuma, and Yumiko Obata

Department of Materials Technology, Faculty of Engineering, Chiba University, Yayoi, Inage, Chiba 263-8522, Japan

Received April 13, 2000; revised August 4, 2000; accepted August 4, 2000

A Cu metal surface was evaluated by a novel technique combining temperature-programmed reduction (TPR) measurement with N_2O oxidation. The technique consists of three steps: the usual TPR measurement, the oxidation of the Cu surface by N_2O, and the subsequent TPR measurement. The surface Cu oxidized by N_2O was determined as a ratio of the peak area of the second TPR profile to that of the first one. It was found that bulk oxidation gradually proceeds after surface oxidation even at 30°C. After the surface oxidation, the Cu_2O produced by N_2O oxidation varied with N_2O exposure time (t) and had a linear correlation with $t^{\frac{1}{2}}$ at temperatures below 100°C. The linear correlation in the parabolic plot proves that bulk oxidation proceeds through the diffusion process, and the Y-intercept corresponds to the surface oxidation. Both the dispersion and the Cu metal surface area of the sample were calculated from the intercept in the parabolic plot for the Cu_2O produced by N_2O oxidation. In addition, we found that a very large Cu metal surface area, as high as 32 $m^2\ g_{cat}^{-1}$, was created on a Cu–MgO catalyst through a citrate process using a molten mixture of copper nitrate, magnesium nitrate, and citric acid.

Key Words: **TPR; N_2O; Cu surface area; bulk; Cu–MgO; citric acid.**

INTRODUCTION

In the oxidation of copper metal, it is known that N_2O oxidizes only the surface (1–3). The surface reaction, $2Cu + N_2O \rightarrow N_2 + Cu_2O$, has been used for the determination of Cu metal surface area of catalyst. In the measurement, consumption of N_2O has been evaluated by volumetric measurement of N_2 produced (1–4), pulse N_2O titration using chromatographic separation (5, 6), and differential heat of N_2O decomposition (1, 7). In classic volumetric measurement under reduced pressures, it takes several hours to accomplish surface oxidation by N_2O (3, 4). In contrast, pulse N_2O titration is convenient for rapid measurement under flow conditions (5, 6). Chinchen *et al.* improved the pulse N_2O titration method by monitoring a change in TCD signal of the N_2O consumption during the N_2O decomposition at 60°C without separating N_2 produced and N_2O unreacted (8). Dandekar and Vannice have recently reported the dispersion and surface oxidation states of supported Cu catalysts using the combination of N_2O decomposition at 90°C and CO adsorption at 27°C (9).

There is some disagreement among several researchers as to the optimum temperature at which Cu surface should be oxidized by N_2O. Scholten and Konvalinka favored performing the N_2O decomposition at 90°C for more reproducible results (3), while Sengupta *et al.* observed a slight increase in the amount of N_2O decomposed with increasing temperature from 30 to 70°C and a sharp increase in the amount of N_2O decomposed due to bulk oxidation above 70°C (4). In pulse titration, Dvořák and Pašek adopted N_2O-oxidation temperatures lower than 60°C (5), whereas Evans *et al.* adopted 90°C (6). As regards the bulk oxidation of Cu, Cu-on-support catalysts are completely oxidized by N_2O at 120°C (2, 3).

Incidentally, we have reported several mixed oxide catalysts such as NiO–MgO (10–13), Fe_2O_3–CeO_2 (14), and CuO–Al_2O_3 (15) prepared by an amorphous citrate process known as a preparation method for fine ceramic powders (16). For example, in NiO–MgO, which forms a solid solution with NaCl-type structure, MgO additives act as an obstacle preventing the aggregation of NiO during the decomposition of the amorphous citrate mixture (12). After the NiO–MgO has been reduced at 500°C, the Ni–MgO catalyst with high Ni content such as 70 wt% had a Ni surface area as high as 30 $m^2\ g^{-1}$ (13). Therefore, we expect that the citrate process in CuO–MgO will provide Cu–MgO with high Cu surface area.

In this paper, we have developed a novel and convenient method for the estimation of Cu surface area using temperature-programmed reduction (TPR) combined with N_2O oxidation, which clearly distinguishes surface and bulk oxidation of Cu. We also estimate Cu surface areas

---

[1] To whom correspondence should be addressed. Fax: +81-43-290-3401. E-mail: satoshi@tc.chiba-u.ac.jp.

0021-9517/00 $35.00

of Cu–MgO catalysts together with other catalysts such as Cu–Al_2O_3 and Cu–SiO_2 by using the present method combining TPR measurement with N_2O oxidation.

EXPERIMENTAL

Pure CuO was prepared from an equimolar molten mixture of copper (II) nitrate trihydrate and citric acid monohydrate. All reagents were supplied by Wako Chemical in Japan. Details of the preparation procedure have been described in the previous papers (10, 12). After the metal citrate precursor had been heated in air at 170°C for 2 h, it was calcined in air at 550°C for 3 h to provide a pure CuO sample. CuO–MgO samples with different copper contents were also prepared using mixtures of copper nitrate, magnesium nitrate, and citric acid. Other reference samples were prepared by either impregnation or the citrate process. The specific surface area (*SA*) of the sample was determined by the BET method using a nitrogen adsorption isotherm measured in a conventional volumetric gas adsorption apparatus at -196°C.

Figure 1 illustrates the TPR apparatus equipped with a N_2O flow line, which is made of stainless tube. A catalyst sample (10–30 mg) was fixed in a glass tube with glass wool, and its temperature was monitored by a thermocouple located outside of the tube. A mixture of H_2/N_2 (=1/9) was flowed at atmospheric pressure with a flow rate of 10 $cm^3\ min^{-1}$, and the consumption of H_2 was detected by a thermal conductivity detector (TCD) cell. N_2O with a flow rate of 1 $cm^3\ min^{-1}$ was introduced into the H_2/N_2 flow: the ratio of $N_2O/H_2/N_2$ was 1/1/9 during the oxidation of Cu. Switching a six-way valve can change the location of the N_2O-injection port for that of the sample bed.

Table 1 summarizes stepwise procedures of the technique. A TPR measurement was done from 30 to 300°C at a heating rate of 10 K min^{-1}, and then the temperature was held at 300°C for 1 h. The first TPR signal was collected (Step 1). It was confirmed that no further reduction peak was observed at higher temperatures. After the first TPR process, the sample was cooled to an N_2O-oxidation temperature, 30–110°C (Step 2). Switching the six-way valve started the oxidation of the reduced sample through contact with N_2O in the H_2/N_2 flow at a prescribed temperature. After a prescribed period, a switch back ended the oxidation of reduced Cu (Step 3). After the TCD signal had been stabilized at the N_2O-oxidation temperature (Step 4), the second TPR was measured from the N_2O-oxidation temperature to 300°C at a heating rate of 10 K min^{-1} to reduce the oxidized Cu surface again (Step 5).

TABLE 1

Stepwise Procedures of the Technique

Step	Procedure
1	Acquisition of **first TPR** signal (A_1) from 30 to 300°C at a heating rate of 10 K min^{-1}
2	Cooling the sample to an N_2O-oxidation temperature
3	**N_2O-oxidation** of the reduced sample at 30–110°C for a prescribed period
4	Stabilization of the TCD signal at the N_2O-oxidation temperature
5	Acquisition of **second TPR** signal (A_2) from the N_2O-oxidation temperature to 300°C

Figure 2 shows typical TPR profiles for pure CuO prepared by the citrate process. The peak area of the first TPR profile (A_1) corresponds to the amount of all CuO in the sample, and that of the second TPR (A_2) is the amount of Cu_2O produced by N_2O oxidation. A fraction of Cu_2O in the total Cu, D^*, is calculated as $D^* = 2A_2/A_1$, which means an apparent Cu dispersion. We calculated D^* using data from a fresh sample because further TPR signal intensity decreased with repeated oxidation–reduction cycles. If N_2O oxidizes only the surface of Cu, D^* is regarded as the true dispersion (D) defined as the ratio of exposed surface Cu to total Cu. Thus, we can calculate the Cu metal surface area per unit weight of catalyst, SA_{Cu}, as SA_{Cu} ($\mathrm{m}^2\ \mathrm{g}_{\mathrm{cat}}^{-1}$) =

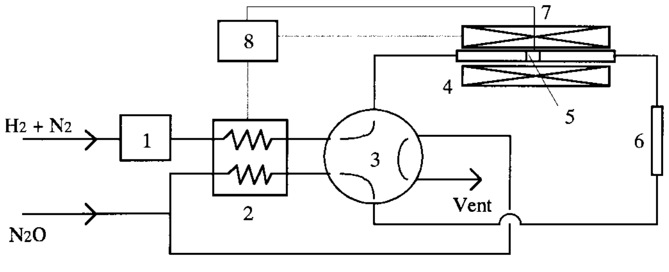

FIG. 1. TPR apparatus and N_2O oxidation flow diagram. 1, Activated Cu operated at 300°C; 2, TCD; 3, six-way valve; 4, furnace; 5, catalyst sample; 6, H_2O adsorption filter filled with molecular sieve 13× and silica gel indicator; 7, thermocouple; 8, PC and temperature controller.

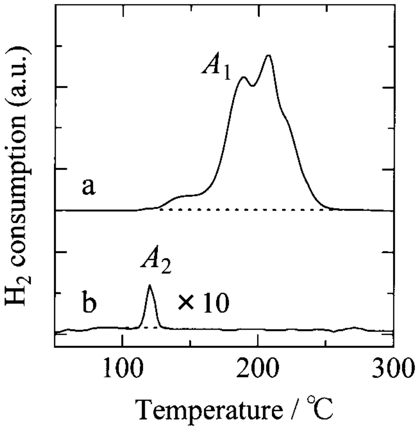

FIG. 2. Typical TPR profiles of pure CuO sample. (a) First TPR; (b) second TPR after N_2O oxidation at 30°C.

$DA_v L_{Cu}/100 W_{Cu} N_A$, where A_v, L_{Cu}, W_{Cu}, and N_A are Avogadro's number, Cu content (wt%) in the catalyst, atomic weight of Cu (63.5 g mol^{-1}), and number of surface Cu atoms in unit surface area, respectively. A reported N_A value, 1.7×10^{19} m^{-2} (17), is used for the calculation of SA_{Cu}, while N_A values in the range (1.68–1.35) $\times 10^{19}$ m^{-2} are available for different Cu crystal planes (7).

RESULTS AND DISCUSSION

Figure 3 shows variations in the fraction of Cu_2O in the total Cu (D^*) with N_2O-exposure time (t) at different temperatures for the pure CuO sample. At any N_2O-oxidation temperatures, the D^* values increased rapidly within 1 min, and they increased gradually with increasing t. The initial increase in the D^* value corresponds to the surface oxidation of Cu by N_2O, and the following one is ascribed to the bulk oxidation. The bulk oxidation proceeds faster at higher temperatures. Even at 30°C, it is obvious that the bulk oxidation gradually proceeds during the continuous contact of N_2O with the surface.

Assuming that the bulk oxidation proceeds through the diffusion process, we can analyze the D^*–t data by using a parabolic plot (18). Thus, the D^* data are replotted against $t^{\frac{1}{2}}$ in Fig. 4. The D^*–$t^{\frac{1}{2}}$ plots fitted with straight lines and had the same Y-intercept at the temperatures below 100°C. The second TPR signals were not reproducible at 110°C. Because the oxidized Cu surface commenced to be reduced at 110°C, as shown in Fig. 2b, both the oxidation of Cu and the reduction of oxidized Cu occur simultaneously. The Y-intercept represents a precise D value for the sample, and then we calculate SA_{Cu} using the D value and Cu content. The D and SA_{Cu} values for the pure Cu sample were 0.0027 and 1.5 m^2 g$_{cat}^{-1}$, respectively. We obtained oxygen coverage 1.15, which is calculated from the specific surface area (SA) of Cu powder prepared by reducing the pure CuO, 1.3 m^2 g$_{cat}^{-1}$. The results indicate another important thing: we had better use D^*–t data to obtain a precise SA_{Cu} value at such a low N_2O-oxidation temperature as 30°C because errors are depressed by the smallest slope of the D^*–$t^{\frac{1}{2}}$ line.

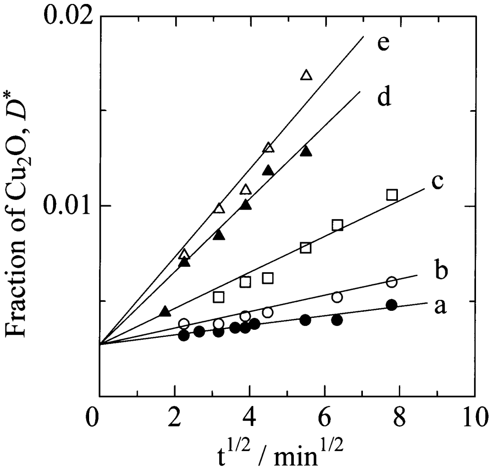

FIG. 4. Parabolic plots for the D^*–t data in Fig. 3. Symbols are the same as those in Fig. 3.

Figure 5 shows D^*–$t^{\frac{1}{2}}$ plots for supported Cu catalysts at the N_2O-oxidation temperature of 30°C. For the Cu–MgO catalysts with Cu content of 30 and 50 wt%, the D^*–$t^{\frac{1}{2}}$ plots also showed linear dependence. D values calculated from the Y-intercepts were 0.156 and 0.117, respectively, and SA_{Cu} values were 26.1 and 32.6 m^2 g$_{cat}^{-1}$, respectively. For Cu-Al_2O_3 with Cu content of 67 wt%, the D^*–$t^{\frac{1}{2}}$ plot also showed a straight line, and the D and SA_{Cu} values were 0.0384 and 14.3 m^2 g$_{cat}^{-1}$, respectively. For

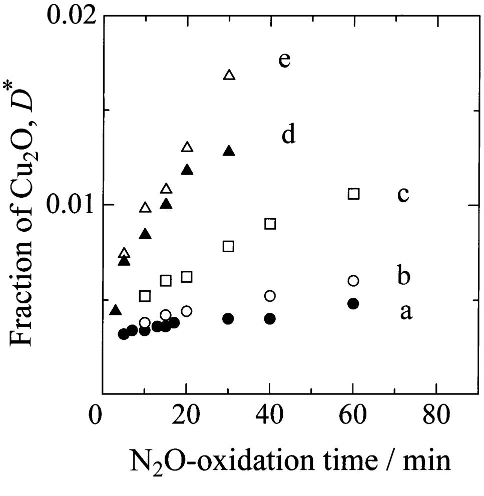

FIG. 3. Variations in D^* with contact time (t) of N_2O at various temperatures for pure CuO. (a) Oxidized by N_2O at 30; (b) 50; (c) 70; (d) 90; (e) 100°C.

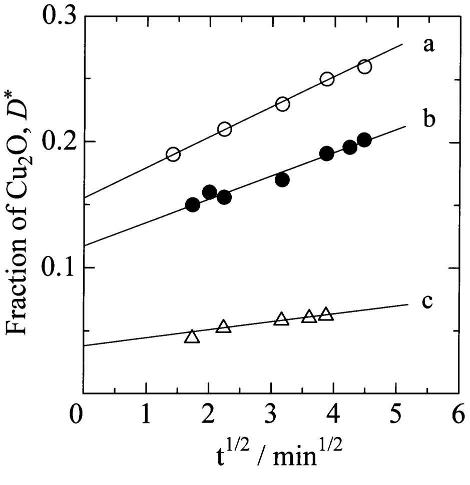

FIG. 5. Parabolic plots for D^*–t data of supported Cu samples. N_2O oxidation at 30°C. (a) Cu(30 wt%)–MgO; (b) Cu(50 wt%)–MgO; (c) Cu(67 wt%)–Al_2O_3.

the Cu(50 wt%)–MgO catalyst, it was also confirmed that D^*–$t^{\frac{1}{2}}$ plots had the same Y-intercept at temperatures of 30, 50, and 70°C.

A D^*/D value corresponds to a thickness of surface Cu_2O layer. At low N_2O-oxidation temperatures such as 30 and 50°C, the D^*/D values were less than 2. Thus, the average width of the bulk Cu_2O layer is thinner than that of the surface oxide monolayer. A Cu ion rather than an oxygen anion is thought to be the diffusion species in the bulk oxidation of Cu particles by O_2 (3). The diffusion of Cu^+ from bulk to surface is probably predominant in the present N_2O oxidation because the size of Cu^+ is smaller than that of O^{2-}. In N_2O exposure above 70°C, the D^*/D values exceed 2 in Figs. 4c–4e, indicating that a bulk Cu_2O overlayer grows on Cu.

When the diffusion process controls the bulk oxidation, the diffusion coefficient depends only on the temperature in the same material (18). In the D^*–$t^{\frac{1}{2}}$ plot, a slope, S, divided by the D obtained is directly concerned with the diffusion coefficient. The S/D values in Fig. 4 are strongly dependent on the temperature. All the S/D values of the supported Cu samples in Fig. 5 were the same, 0.16 $min^{-\frac{1}{2}}$, while the S/D of the pure Cu sample in Fig. 4a was 0.09 $min^{-\frac{1}{2}}$ at 30°C. The same values with different samples suggest that bulk oxidation through diffusion proceeds at the same rate in the supported Cu catalysts. Osinga *et al.* reported that bulk oxidation of Cu powder needed a temperature about 20 K higher than that for supported Cu catalysts (2). Since the S/D value for the pure CuO is smaller than that of supported Cu samples, it is speculated that the diffusion process depends on the Cu particle size.

The time dependence of D^* depicted in Fig. 3 is different from the kinetic data that Scholten and Konvalinka measured for pure Cu, where it takes several hours to perform the decomposition of N_2O under reduced pressure (Fig. 2 in Ref. 3). The difference is probably due to the different total pressures. In contrast, the pulse N_2O titration reported by Evans *et al.* realizes Cu surface oxidation even in a short contact time with Cu under N_2O flow at atmospheric pressure (6). The measurement conditions are similar to the present ones, while the difference is whether surface oxide is directly detected or not. In our preliminary pulse N_2O titration experiment over Cu–MgO at 90°C, we observed that N_2O decomposed even after several pulses of N_2O, as has been reported in Table 2 in Ref. (6). If we assume bulk oxidation, we can explain the increase in the N_2O consumption through the multiple pulses of N_2O.

Since no hydrogen liberation was observed in the second TPR without N_2O oxidation, hydrogen adsorbed can be negligible at 30°C. Thus, the reaction of surface hydrogen atoms with N_2O during the oxidation would not invalidate the Cu surface area calculation. In addition, even at a high N_2O partial pressure with $N_2O/H_2/N_2 = 2/1/9$ in the oxidation, the same D value was observed for a CuO–MgO sample at 30°C. Although the temperature measured is not always the same as the surface temperature, the possibility of surface heating invalidating the temperature measurement can be denied because there is no influence of N_2O partial pressure on the present N_2O oxidation.

TABLE 2

Physical Properties of Cu–MgO and Other Reference Samples

Sample	Cu content (wt%)	D^a (−)	$SA_{Cu}{}^a$ ($m^2\ g_{cat}^{-1}$)	SA^b ($m^2\ g_{cat}^{-1}$)
Cu–MgO[c]	20	0.180	20.1	84.3
	30	0.156	26.1	71.6
	50	0.117	32.6	62.4
	60	0.0643	21.5	45.2
	100	0.0027	1.5	1.3
$Cu–Al_2O_3$[c]	46	0.0275	7.1	105
	67	0.0384	14.3	100
$Cu-SiO_2$[d]	20	0.0269	3.0	236

[a] Measured by the present method through N_2O oxidation at 30°C.

[b] Measured by BET method for the unreduced sample.

[c] Prepared by citrate process, sample was calcined at 550°C.

[d] Prepared by impregnation method using copper nitrate, sample was calcined at 550°C.

Table 2 summarizes physical properties of Cu–MgO catalysts. In the Cu–MgO samples, SA_{Cu} exhibited a maximum at a Cu content of 50 wt%, while both D and specific surface area (SA) monotonically decreased with increasing Cu content. It was found that Cu metal surface occupied about half of the specific surface area in the Cu(50 wt%)–MgO sample. The prereduced CuO–MgO sample was a mixture of CuO and MgO as speculated from XRD data (not shown), in contrast to the case of NiO–MgO, which consists of a solid solution and has a maximum Ni surface area at 70 wt% Ni (12). We also tested other reference catalysts, as listed in Table 2. Cu(20 wt%)/SiO_2, prepared by impregnating $Cu(NO_3)_2$aq on SiO_2 gel (specific surface area 295 $m^2\ g^{-1}$), and $Cu–Al_2O_3$, prepared by the citrate process, had SA_{Cu} less than 14.3 $m^2\ g_{cat}^{-1}$ even on a high-surface-area support.

In conclusion, we have developed a new technique, a back titration of surface Cu_2O with H_2, which combines a TPR experiment with N_2O oxidation to estimate Cu metal surface area. The technique consists of three steps: a standard TPR measurement, oxidation of Cu by N_2O, and a subsequent TPR. The fraction of Cu_2O produced by N_2O oxidation out of the total Cu was calculated as the ratio of the TPR peak area of the second TPR profile to the first one. The fraction of Cu_2O varied with N_2O exposure time (t) and had a linear correlation with $t^{\frac{1}{2}}$ at temperatures below 100°C. The linear correlation in the parabolic plot proves that bulk oxidation proceeds through the diffusion process. The Y-intercept in the parabolic plot corresponds to the surface Cu_2O, which means true dispersion of Cu. Although bulk oxidation proceeds gradually after surface oxidation even at 30°C, the Cu metal surface area of sample are calculated by the true dispersion and Cu content. The technique is powerful for estimating Cu surface area under the conditions where the catalyst support is not reduced in the TPR process. We additionally found that a Cu–MgO catalyst with Cu surface area as high as 32 $m^2\ g_{cat}^{-1}$ colud be prepared through a citrate process using a molten mixture of copper nitrate, magnesium nitrate, and citric acid.

REFERENCES

1. Dell, R. M., Stone, F. S., and Tiley, P. F., *Trans. Faraday Soc.* **49**, 195 (1953).
2. Osinga, Th. J., Linsen, B. G., and van Beek, W. P., *J. Catal.* **7**, 277 (1967).
3. Scholten, J. J. F., and Konvalinka, J. A., *Trans. Faraday Soc.* **65**, 2465 (1969).
4. Sengupta, G., Gupta, D. K., Kundu, M. L., and Sen, S. P., *J. Catal.* **67**, 223 (1981).
5. Dvořák, B., and Pašek, J., *J. Catal.* **18**, 108 (1970).
6. Evans, J. W., Wainwright, M. S., Bridgewater, A. J., and Young, D. J., *Appl. Catal.* **7**, 75 (1983).
7. Giamello, E., Fubini, B., Lauro, P., and Bossi, A., *J. Catal.* **87**, 435 (1984).
8. Chinchen, G. C., Hay, C. M., Vandervel, H. D., and Waugh, K. C., *J. Catal.* **103**, 79 (1987).
9. Dandekar, A., and Vannice, M. A., *J. Catal.* **178**, 621 (1998).
10. Sato, S., Nozaki, F., and Nakayama, T., *Appl. Catal. A* **139**, L1 (1996).
11. Nakayama, T., Yamashiro, K., Sato, S., and Nozaki, F., *Appl. Catal. A* **151**, 437 (1997).
12. Nakayama, T., Ichikuni, N., Sato, S., and Nozaki, F., *Appl. Catal. A* **158**, 185 (1997).
13. Sato, S., Takahashi, R., Sodesawa, T., Nozaki, F., Jin, S.-Z., Suzuki, S., and Nakayama, T., *J. Catal.* **191**, 261 (2000).
14. Kamimura, Y., Sato, S., Takahashi, R., Sodesawa, T., and Fukui, M., *Chem. Lett.* 232 (2000).
15. Sato, S., Iijima, M., Nakayama, T., Sodesawa, T., and Nozaki, F., *J. Catal.* **169**, 447 (1997).
16. Marcilly, C., Courty, P., and Delmon, B., *J. Am. Ceram. Soc.* **53**, 56 (1970).
17. Sundquist, B. E., *Acta Met.* **12**, 67 (1964).
18. Kingery, W. D., Bowen, H. K., and Uhlmann, D. R., *in* “Introduction to Ceramics,” 2nd ed., Chap. 6, p. 217, Wiley, New York, 1976.